New Luminescent Tetranuclear Lanthanide-based Silsesquioxane Cage-like Architectures

Alena N. Kulakova, Alexey N. Bilyachenko, Mikhail M. Levitsky, Victor N. Khrustalev, Elena S. Shubina, Gautier Félix, Ekaterina Mamontova, Jérôme Long, Yannick Guari, Joulia Larionova

New Luminescent Tetranuclear Lanthanide-based Silsesquioxane Cage-like Architectures

Alena N. Kulakova,[a],[b],[c] Alexey N. Bilyachenko,*[a],[b] Mikhail M. Levitsky,[a] Victor N. Khrustalev,[b],[d] Elena S. Shubina,[a] Gautier Felix,[c] Ekaterina Mamontova,[c] Jérôme Long,[c] Yannick Guari,[c] and Joulia Larionova*[c]

[a] A.N. Kulakova, Dr. A.N. Bilyachenko, Dr. M.M. Levitsky, Prof. E.S. Shubina
Nesmeyanov Institute of Organoelement Compounds, Russian Academy of Sciences
Vavilova str., 28, Moscow, 119991, Russia
E-mail: bilyachenko@ineos.ac.ru

[b] A.N. Kulakova, Dr. A.N. Bilyachenko, Prof. V.N. Khrustalev
Peoples' Friendship University of Russia
Miklukho-Maklay Str., 6, 117198, Moscow, Russia

[c] A.N. Kulakova, Dr. G. Felix, E. Mamontova, Dr. J. Long, Dr. Y. Guari, Prof. J. Larionova
ICGM, Univ. Montpellier, CNRS, ENSCM, Montpellier, France,
E-mail: joulia.larionova@umontpellier.fr

[d] Prof. V.N. Khrustalev
Zelinsky Institute of Organic Chemistry, Russian Academy of Sciences
Leninsky Prospect 47, Moscow 119991, Russia

Abstract: We report on the synthesis, structure, magnetic and luminescence properties investigations of four new cage-like lanthanide-based silsesquioxanes $(Cat)_2[(PhSiO_{1.5})_8(LnO_{1.5})_4(O)(NO_{2.5})_6(EtOH)_2(MeCN)_2]$ (where $Cat^+ = Et_4N^+$, PPh_4P^+ and $Ln^{3+} = Eu^{3+}$ Tb^{3+} and $(Ph_4P)_4[(PhSiO_{1.5})_8(TbO_{1.5})_4(O)_2(NO_{2.5})_8]$•10MeCN. They present an unusual prism-like topology of cage architectures and lanthanide-characteristic emission, which makes them the first luminescent cage-like lanthanide silsesquioxanes. One of the Tb^{3+}-based cages presents a magnetic spin-flip transition.

Cage-like metallasilsesquioxanes (CLMSs) belong to an intensively developed family of molecule-based architectures, which is widely investigated due to their original structures of surprising topological diversity and their physical and chemical properties, including catalytic activity, porosity, stability, host-guest chemistry and magnetism.[1] These compounds benefit from the advantages of coordination and sol-gel chemistries and are often referred as versatile hybrid organic-inorganic materials.[2] They are members of a more wide class of polynuclear cages [3] and their particularity consists in the presence of silsesquioxane ligands, $(RSiO_{1.5})_n$ (where n = 6, 8, 10, 12), forming inorganic Si-O-Si skeletons as a basic structural unit, which connect metal, lanthanide or actinide ions through their coordination to oxygen atoms to assemble them into robust polynuclear cages.[4] Moreover, these latter may be functionalized by different organic moieties usually located on the cages' peripheries. Whereas different types of siloxane-based skeletons bring to these architectures the mechanical robustness, chemical stability, protection and possibility to form cage-like topology, the presence of metal ions is also crucial considering their valuable physical properties.[5] Thus, various *s-block* metal ions and transition metal ions, including $Pt^{2+/4+}$, Cr^{3+}, Mn^{2+}, Ti^{3+}, Fe^{3+}, Ni^{2+}, Cu^{2+} or their combinations have largely been employed for the design of polynuclear CLMSs of different topology, such as adamantane, cooling tower, birdcage, cube, drum, sandwich-like, Asian lantern and others.[2b, 4a] CLMS architectures have mainly been investigated for their catalytic properties making them interesting as molecular models for catalysis applications and offering a unique opportunity to understand heterogeneous catalysis at a molecular level.[6] In general, they not only demonstrated a high activity and selectivity in comparison to classical catalysts, but also show an improved stability regarding the number of repeated catalytic cycles. On the other hand, some polynuclear CLMSs containing paramagnetic transition metal ions, such as Co^{2+}, Ni^{2+}, Cu^{2+} or $Fe^{3+/2+}$, have also been investigated

for their unusual magnetic properties consisting in the appearance of a slow relaxation of the magnetization induced by a spin-glass or single molecule magnet behaviour.[7]

Surprisingly, the number of works devoted to design of CLMSs involving lanthanide ions are relatively scarce despite the great interest to their employment in molecule-based materials. Indeed, lanthanide-based complexes of different nuclearity and their extended structures saw a huge development in the recent years owing to exceptional magnetic and optical properties allowing an emergence or progress of interesting physical phenomena and related applications including a high temperature slow relaxation of the magnetization in mononuclear lanthanide Single Molecule Magnets,[8] lanthanide-based luminescence,[9] magnetoelectric materials,[10] luminescent thermometry,[11] optical labelling,[12] Magneto Resonance Imaging,[13] catalysis[14] and others. However, to the best of our knowledge, only two families of lanthanide-based CLMSs have been reported in the literatures up to now. Firstly, there is a series of cages with three cyclic siloxane moieties assembled through cubane-like core containing lanthanide ions (Yb^{2+}, Yb^{3+}, Nd^{3+}, Er^{3+}, Ce^{3+}, Eu^{3+}, Sm^{3+} or Pr^{3+}).[15] Secondly, we can cite also tetrameric silsesquioxane cages (with La^{3+}, Nd^{3+}, Gd^{3+} or Dy^{3+})[16] presenting a sandwich-like structure, where the tetranuclear oxo-lanthanide core is caught between two siloxane moieties. Note that the Tb^{3+}- containing CLMSs have never been reported up to now. Moreover, all these lanthanide-containing CLMSs have been regarded especially as model compounds for catalysis[15a-f, 15h] or components of catalytic systems. [15g] Yet, their optical and magnetic properties have never been investigated. We can cite only one study reporting on the occurrence of an emission in a mononuclear Eu^{3+} based CLMSs, but its crystal structure has not been elucidated.[15j]

In the present communication, we report on a series of new tetranuclear Eu^{3+}- and Tb^{3+}-based CLMSs presenting an unusual prism-like topology of cages. Note that our Tb^{3+} compounds constitute the first example of Tb^{3+} based CLMSs. All reported compounds present a lanthanide-characteristic luminescence making them the first luminescent CLMSs. The investigation of their magnetic properties reveals the presence of a magnetic spin-flip behavior for one of the Tb^{3+} analogue.

The synthesis of lanthanide-based CLMSs has been performed by using a two-step reaction involving, first, the *in-situ* formation of phenylsiloxanolate $[PhSi(O)ONa]_x$ species with their following self-assembling reaction with the corresponding lanthanide nitrates and tertiary ammonium Et_4NCl or phosphonium Ph_4PCl salts (Scheme 1, see ESI for details). The crystallization from an acetonitrile/ethanol mixture affords single crystals of the four compounds $(Cat)_2[(PhSiO_{1.5})_8(LnO_{1.5})_4(O)(NO_{2.5})_6(EtOH)_2(MeCN)_2]$ (where $Cat^+ = Et_4N^+$, $Ln^{3+} = Eu^{3+}$ (**1**), $Cat^+ = Ph_4P^+$, $Ln^{3+} = Eu^{3+}$ (**2**), $Cat = Et_4N^+$, $Ln^{3+} = Tb^{3+}$ (**3**) and $(Ph_4P)_4[(PhSiO_{1.5})_8(TbO_{1.5})_4(O)_2(NO_{2.5})_8]$•10MeCN (**4**).

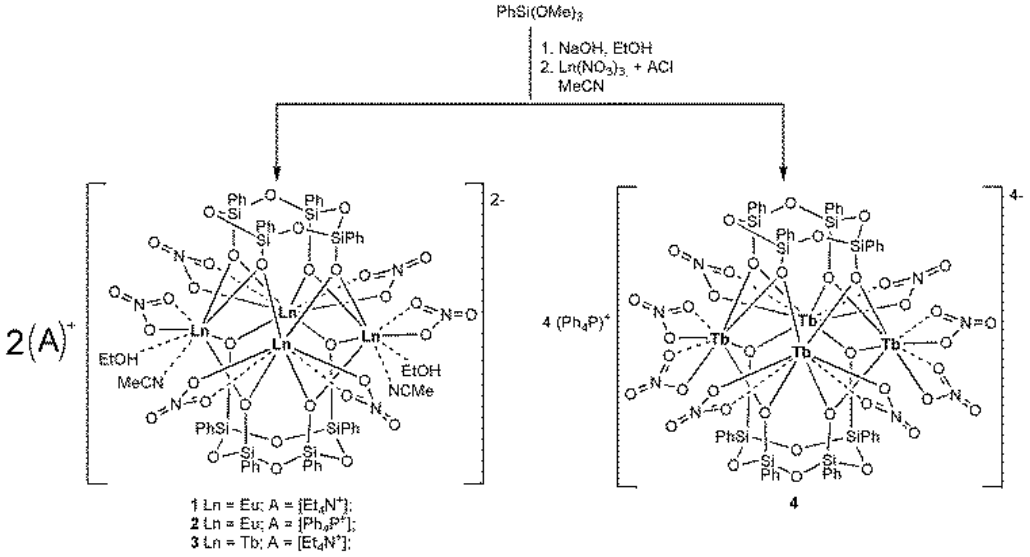

Scheme 1. Synthesis of lanthanide-based CLMSs **1** – **4**.

X-Ray diffraction analysis indicates that compounds **1** – **3** crystalize in the triclinic *P-1* space group and present closed crystal structures. On the other hand, compound **4** crystallizes in *P2$_1$/c* space group, but its molecular architecture is also similar to the others. The structural description for only **1** will be given in details.

The molecular structure of the cage **1** may be viewed as a prism made by tetranuclear core situated in the middle, which is sandwiched by two *cisoid* cyclic tetraphenylcyclotetrasiloxanolate moieties (Fig. 1a, b). Note that such tetrameric ligands is quite rare for cage metallasilsesquioxanes, which has been earlier reported only for tetranuclear titanium-based CLMS[17] and octanuclear cobalt-based silsesquioxanes.[18] Each Eu^{3+} ion is linked to two others through two bridging oxygen atoms to form a distorted square. There are two different Eu sites in the structure, both of them being eight coordinated. One is coordinated by four bridging oxygen atoms from $(EuO_2)_4$ core and four oxygen atoms from two terminal bidentate nitrate ligands, while another one is linked to four bridging oxygens, two terminal oxygens from one nitrate, one ethanol and one acetonitrile molecules (Fig. 1b). The Eu-O distances are in the range 2.341 – 2.357 Å, while the Eu-N one is equal to 2.572 Å. The O-Eu-O angles in the square are equal to 81.02 and 119.77°. The geometry of both sites maybe described as distorted square antiprisms. The intramolecular Eu^{3+}-Eu^{3+} distances are equal to 3.744 and 3.791 Å. The view of the crystal packing of **1** along the *b* axis indicates that the tetranuclear di-anions are arranged in the same way, namely, their molecular axes (the normal to the Eu_4-plane) are directed practically along the crystallographic *b* axis, whereas the disposition of cations is different (Fig. S1, ESI). The shortest intermolecular Eu-Eu distance is equal to 7.954 Å. The molecular structures of **2** and **3**, their crystal packings, as well as the relevant distances and angles are summarized in ESI (Fig. S2 – S5, ESI).

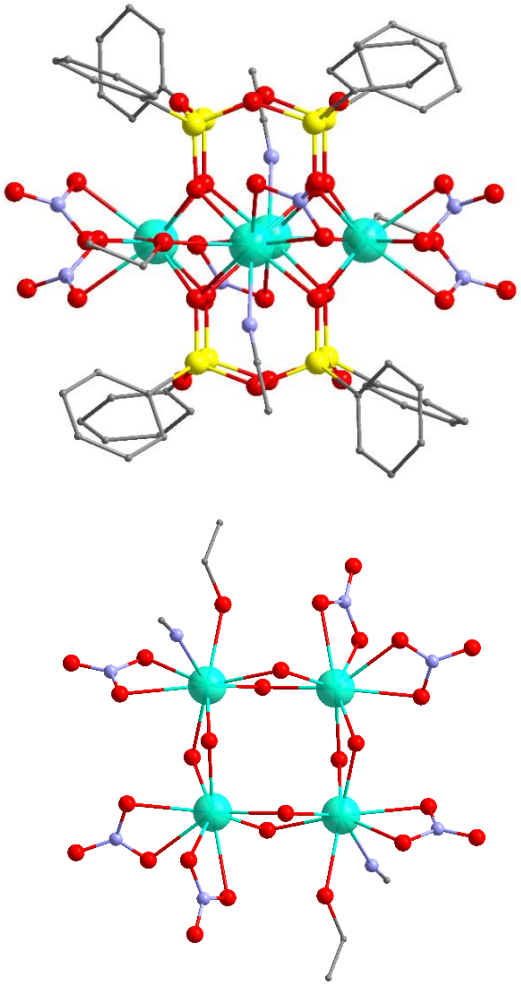

Figure 1. Top) Molecular structure of **1**. Hydrogen atoms and crystallized ethanol and acetonitrile molecules have been omitted for clarity; Bottom) Representation $(EuO_2)_4$ core of **1** showing the coordination geometry of Eu sites. Color code: cyan, Eu; yellow, Si; red, O; blue, N, grey C.

The terbium containing compound **4** presents a similar topology but (Fig. S6, ESI), the electroneutrality is assured by four Ph_4P^+ cations. Although there are two crystallographically independent Tb sites, their environment is identical in contrast to **1-3**: they are coordinated by four bridging oxygen atoms and four oxygens from two terminal nitrates (Fig. S6, ESI). The crystal packing showed in Fig. S7 along the *a* axis indicates that the molecular axes of tetranuclear terbium tetra-anions are directed almost toward the main diagonals of the unit cell. Note that the shortest intermolecular Tb-Tb distance of 12.211 Å is much larger in comparison to the one in **3** (7.997 Å) due to the bulky counter cation permitting a better isolation of the cages.

Since the Eu^{3+} containing CLMSs **1** and **2** are diamagnetic at low temperature, the magnetic properties of Tb^{3+} based CLMSs **3** and **4** were investigated by using a SQUID MPMS-XL magnetometer working between 1.8 – 300 K and up to 7 T.

The temperature dependence of the magnetic susceptibility performed in direct current (dc) mode has been performed under an applied magnetic field of 1000 Oe. The room temperature χT values of 46.10 and 44.10 $cm^3.K.mol^{-1}$ for **3** and **4** are slightly lower in comparison with the theoretical value expected for four Tb^{3+} ions of 47.28 $cm^3.K.mol^{-1}$ using the free-ion approximation ($^7F_6$, S = 3, L = 3, g = 3/2, χT = 11.82 $cm^3.K.mol^{-1}$).[19] Upon cooling, the compounds exhibit the typical decrease of χT caused by the thermal depopulation of the Stark sublevels and/or the presence of antiferromagnetic interactions between the Tb^{3+} centers (Fig. S8A, ESI).

The field dependences of the magnetization performed at 1.8 K show a S-shape curve for **3** suggesting the presence of a spin flip of magnetic moment related to different Tb^{3+} ions in antiferromagnetic interaction under an applied magnetic field,[19a, 20] while a linear increase of the magnetization with field at low fields is observed for **4** (Fig. S8B, ESI). Both curves never reach the saturation and the magnetisation values of 19.10 and 21.37 $N\beta$ under 70 kOe field for **3** and **4**, respectively, indicate the presence of a significant magnetic anisotropy. The M *vs* H curves for **3** performed for different temperatures indicate the dissapearence of the sigmoidal shape at 6 K (Insert of Fig. S8B). The H *vs* T phase diagram (Fig. S8C) drawn from the maxima of the dM/dH curves performed at different temperatures demarcates the domain of the spin cating regim from the oriented paramagnetic one.

The dynamic magnetic measurements performed in the alternating currents (ac) mode were conducted to probe the spin flip behavior. Under a zero-dc field, the in-phase component of the magnetic susceptibility (χ') shows a frequency independent peak at 3.32 K, while the out-of-phase susceptibility (χ'') component is almost zero and shows a little increase at 1.8 K (Fig. S9A, ESI). This former depends on an applied magnetic field and progressively shifts towards lower temperatures as the field increases and disappeared at 3000 Oe (Fig. S9B, ESI). Note that the difference in magnetic behavior between **3** and **4** may be due to : (*i*) the presence of two Tb sites with different coordination environement in **3**, which might generate different orientation of the anisotropy axes that may explain the spin canting regime at low field, and (*ii*) stronger intermolecular interactions in **3** explained by a relatively close intermolecular Tb…Tb distances of 7.954 Å, in comparison with 12.211 Å in **4**, where the cages are better isolated.

The photoluminescence of **1** - **4** has been investigated in solid state at 298 and 77 K (Fig. 2, Fig. S10-S18, ESI). For all CLMSs, the excitation in the UV or blue regions results in the typical emission of the constitutive lanthanide ion, Eu^{3+} or Tb^{3+}.

The emission spectra of **1** and **2** performed at 77K are formed of the Eu^{3+} intra-$^4f_6$ lines attributed to the $^5D_0 \rightarrow {}^7F_{0\text{-}4}$ transitions (Fig. 2 top, Fig. S10-S11, S13 ESI).The very weak $^5D_0 \rightarrow {}^7F_0$ transition observed at 579 nm confirms the low symmetry of the coordination environment of the Eu^{3+} sites, while a symmetric shape of this band suggests a relatively the small differences in the Eu-O bond length and angles of the two europium sites, in accordance with the crystal structure [21]

The existence of more than three lines for the $^5D_0 \rightarrow {}^7F_1$ transition is also coherent with the presence of two europium sites in distorted square antiprism geometry. However, the origin of these additional peaks from vibronic satellites also can not be excluded. As expected for compounds with low symmetry europium sites, the $^5D_0 \rightarrow {}^7F_2$ transition dominates

the emission spectra and is responsible of compounds' red emission. The presence of slightly different coordination environement of two Eu^{3+} sites is also corroborated with the splitting of the $^5D_0 \rightarrow {}^7F_2$ and $^5D_0 \rightarrow {}^7F_4$ electronic transitions, which are sensitive to the symmetry of the coordination environment.[21] In order to get further insight into the Eu^{3+} local coordination, the energy, E_{00}, and the full-width-at-half-maximum, $fwhm_{00}$, of the non-degenerated $^5D_0 \rightarrow {}^7F_0$ transition was estimated. Similar E_{00} values, 17248.5 ± 0.1 and 17250.6 ± 0.1 cm^{-1}, was found for the **1** and **2**, respectively, pointing out closed Eu^{3+} coordination sphere in both compounds. The high $fwhm_{00}$ values, namely 21.9 ±0.1 and 20.4.± 0.3 cm^{-1} for **1** and **2**, respectively, are compatible with the presence of different Eu^{3+} local environments [21].The characteristic Tb^{3+}- luminescence could be observed on the emission spectra of **3** and **4** recorded at 77 K with emission peaks assigned to intra-$^4f_8$ $^5D_4 \rightarrow {}^7F_{6\text{-}0}$ transitions (Fig. 2 bottom, Fig. S10, S15, S17 ESI). The most intense emission is centered at 543 nm for both cages, which corresponds to the $^5D_4 \rightarrow {}^7F_5$ transition.

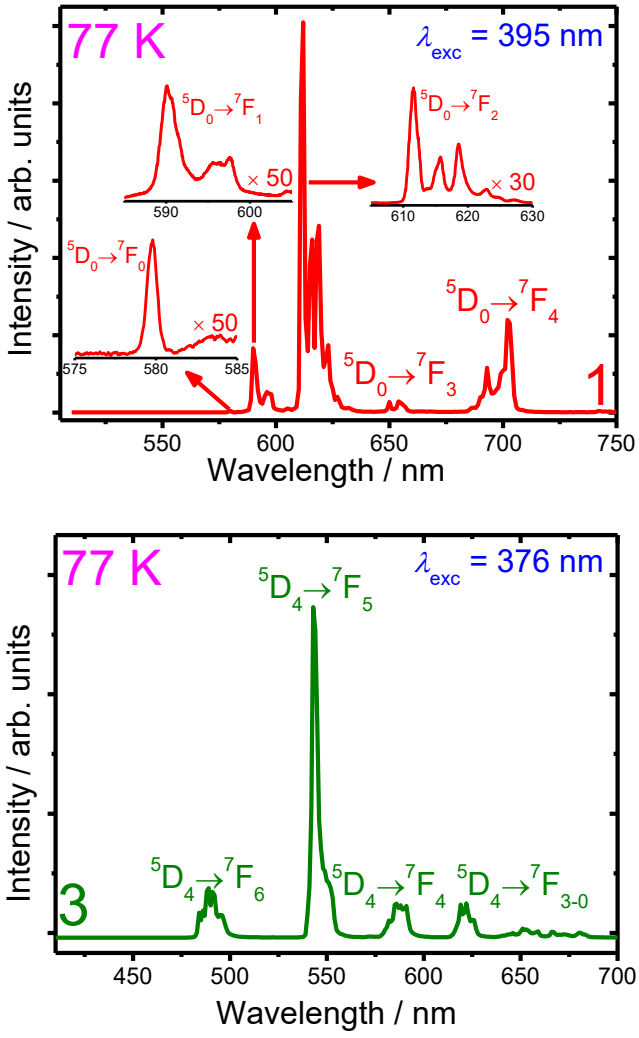

Figure 2. Low temperature (77 K) emission spectra of: (Top) **1** excited at 394 nm. Insert: High-resolution emission spectra for the $^5D_0 \rightarrow {}^7F_{0\text{-}2}$ transitions; (Bottom) **3** excited at 376 nm.

Note that for all compounds, besides an intensity decrease, the room temperature emission and excitation features resemble to those acquired at 77 K (Fig. S10-S18, ESI).

Fig. S12 and S14 show the excitation spectra for **1** and **2** monitored within the $^5D_0 \rightarrow {}^7F_2$ transition (at 77 K). Both of them display a series of straight lines, which could be ascribed to the intra-$4f^6$ transitions $^7F_0 \rightarrow {}^5D_{4\text{-}0}$, $^5L_{8\text{-}6}$, $^5G_{6\text{-}2}$, $^5F_3$, $^6F_1$, $^6H_5$, $^6K_6$. [22] The excitation spectra for compounds **3** and **4** monitored within $^5D_4 \rightarrow {}^7F_5$

transition exhibit a series of sharp Tb^{3+} lines (Fig. S16, S18, ESI), ascribed to the intra $4f^8$ transitions between the $^7F_6$ and the $^5G_{4\text{-}6}$, $^5L_{9\text{-}10}$, $^5D_{1\text{-}3}$, $^5H_7$ levels. [23] Consequently, the absence of broad bands related to the ligand in the excitation spectra of all compounds clearly points out a direct sensitization of the lanthanide ions through *f-f* transitions rather than an energy transfer involving the ligands. Thus, though they do not act as a sensitizer, the siloxane and coordinated nitrate and solvate molecules do not quench the Eu^{3+} and Tb^{3+} emission.

The emission decay curves of cages **1 – 4** were monitored in solid state at 295 K within the $^5D_0 \rightarrow {}^7F_2$ transition for **1** and **2** and within $^5D_4 \rightarrow {}^7F_5$ one for **3** and **4**, respectively. The curves are well reproduced by single exponential functions and allow to determine the luminescence lifetimes. They are equal to 0.777 ± 0.003 and 0.692 ± 0.010 ms for **1**, **2** and 1.742 ± 0. 012 and 1.818 ± 0.01 ms for **3** and **4**, respectively (Fig. S19 – 22, ESI), which are typical values for europium and terbium complexes.[21b, 24]

In summary, four new Eu^{3+} and Tb^{3+} -based CLMS architectures have been synthesized and their magnetic and luminescent properties have been investigated. They present unusual prism-like topology of cages with four lanthanide ions linked through oxygen atoms and situated between two cyclic tetraphenylcyclotetrasiloxanolate moieties. The investigation of the magnetic properties reveals that one of the Tb^{3+}-based cages presents a field induced spin-flip transition from the spin canted state to the oriented paramagnetic regime. Remarkably, these compounds present Eu^{3+} or Tb^{3+}-characteristic luminescence at low and room temperatures and may be considered as first luminescent lanthanide-based CLMSs.

Acknowledgements

This work was supported by the RSF (project 17-73-30036). J. La., Y. G. and J. Lo. thank the University of Montpellier and CNRS for financial support (project PRC2287 Premium 2019-2021). Authors are grateful to Platform of Analysis and Characterization (PAC) of ICGM for magnetic and X-Ray diffraction measurements. J.La. is grateful for Vernadski program (Embassy of France in Russian Federation). ANB is grateful to Dr. Aleksei A. Titov (INEOS RAS) for the fruitful discussion of this work. Elemental analyses were performed with the financial support from the Ministry of Science and Higher Education of the Russian Federation and using the equipment of the Center for Molecular Composition Studies of INEOS RAS.

Keywords: Cage-like metallasilsesquioxanes • Lanthanides • Luminescence • europium • terbium

[1] a) V. Lorenz, F. T. Edelmann, *Metallasilsesquioxanes Adv. Organomet. Chem., Vol. 53*, **2005 53, 101–153**; b) M. M. Levitsky, B. G. Zavin, A. N. Bilyachenko, *Russ. Chem. Rev.* **2007**, *76*, 847-866.

[2] a) R. Murugavel, A. Voigt, M. G. Walawalkar, H. W. Roesky, *Chem. Rev.* **1996**, *96*, 2205-2236; b) H. W. Roesky, G. Anantharaman, V. Chandrasekhar, V. Jancik, S. Singh, *Chemistry-A European Journal* **2004**, *10*, 4106-4114.

[3] a) Z. Wang, H.-F. Su, Y.-Z. Tan, S. Schein, S.-C. Lin, W. Liu, S.-A. Wang, W.-G. Wang, C.-H. Tung, D. Sun, L.-S. Zheng, *Proceedings of the National Academy of Sciences* **2017**, *114*, 12132-12137; b) W. Muhammad, J. Ni, Z. Jagličić, P. Cui, L. Gao, D. Sun, *Chin. Chem. Lett.* **2**020, doi.org/10.1016/j.cclet.2020.01.031; c) K. Sheng, X. Tian, M. Jagodič, Z. Jagličić, N. Zhang, Q.-Y. Liu, C.-H. Tung, D. Sun, *Chin. Chem. Lett.* **2020**, *31*, 809-812.

[4] a) M. M. Levitsky, A. N. Bilyachenko, *Coord. Chem. Rev.* **2016**, *306*, 235-269; b) V. Lorenz, A. Fischer, S. Gießmann, J. W. Gilje, Y. Gun'ko, K. Jacob, F. T. Edelmann, *Coord. Chem. Rev.* **2000**, *206-207*, 321-368.

[5] a) M. M. Levitsky, Y. V. Zubavichus, A. A. Korlyukov, V. N. Khrustalev, E. S. Shubina, A. N. Bilyachenko, *J. Cluster Sci.* **2019**, *30*, 1283-1316; b) F. Edelmann, P. Jutzi, U. Schubert, *Silicon Chemistry: From the Atom to Extended Systems*, Jutzi, P., Schubert, U., Eds, **2007, 383–394**.

[6] a) A. J. Ward, A. F. Masters, T. Maschmeyer, in *Applications of Polyhedral Oligomeric Silsesquioxanes* (Ed.: C. Hartmann-Thompson), Springer Netherlands, Dordrecht, **2011**, pp. 135-166; b) M. Levitskii, V. Smirnov, B. Zavin, A. Bilyachenko, A. Y. Rabkina, *Kinetics and Catalysis* **2009**, *50*, 490-507; c) M. M. Levitsky, A. I. Yalymov, A. N. Kulakova, A. A. Petrov, A. N. Bilyachenko, *J. Mol. Catal. A: Chem.* **2017**, *426*, 297-304; d) M. M. Levitsky, A. N. Bilyachenko, G. B. Shul'pin, *J. Organomet. Chem.* **2017**, *849-850*, 201-218.

[7] a) Y.-N. Liu, J.-L. Hou, Z. Wang, R. K. Gupta, Z. Jagličić, M. Jagodič, W.-G. Wang, C.-H. Tung, D. Sun, *Inorg. Chem.* **2020**, *59*, 5683-5693; b) M. M. Levitsky, A. N. Bilyachenko, E. S. Shubina, J. Long, Y. Guari, J. Larionova, *Coord. Chem. Rev.* **2019**, *398*, 213015; c) A. N. Bilyachenko, A. I. Yalymov, A. A. Korlyukov, J. Long, J. Larionova, Y. Guari, Y. V. Zubavichus, A. L. Trigub, E. S. Shubina, I. L. Eremenko, *Chemistry–A European Journal* **2015**, *21*, 18563-18565; d) A. N. Bilyachenko, A. I. Yalymov, A. A. Korlyukov, J. Long, J. Larionova, Y. Guari, A. V. Vologzhanina, M. A. Es' kova, E. S. Shubina, M. M. Levitsky, *Dalton Trans.* **2016**, *45*, 7320-7327; e) A. N. Bilyachenko, M. M. Levitsky, A. I. Yalymov, A. A. Korlyukov, A. V. Vologzhanina, Y. N. Kozlov, L. S. Shul'pina, D. S. Nesterov, A. J. L. Pombeiro, F. Lamaty, X. Bantreil, A. Fetre, D. Liu, J. Martinez, J. Long, J. Larionova, Y. Guari, A. L. Trigub, Y. V. Zubavichus, I. E. Golub, O. A. Filippov, E. S. Shubina, G. B. Shul'pin, *RSC Advances* **2016**, *6*, 48165-48180; f) A. N. Bilyachenko, M. M. Levitsky, A. I. Yalymov, A. A. Korlyukov, V. N. Khrustalev, A. V. Vologzhanina, L. S. Shul'pina, N. S. Ikonnikov, A. E. Trigub, P. V. Dorovatovskii, X. Bantreil, F. Lamaty, J. Long, J. Larionova, I. E. Golub, E. S. Shubina, G. B. Shul'pin, *Angew. Chem. Int. Ed.* **2016**, *55*, 15360-15363; g) A. N. Bilyachenko, A. Yalymov, M. Dronova, A. A. Korlyukov, A. V. Vologzhanina, M. A. Es'kova, J. Long, J. Larionova, Y. Guari, P. V. Dorovatovskii, E. S. Shubina, M. M. Levitsky, *Inorg. Chem.* **2017**, *56*, 12751-12763.

[8] a) D. N. Woodruff, R. E. P. Winpenny, R. A. Layfield, *Chem. Rev.* **2013**, *113*, 5110-5148; b) F.-S. Guo, B. M. Day, Y.-C. Chen, M.-L. Tong, A. Mansikkamäki, R. A. Layfield, *Science* **2018**, *362*, 1400-1403; c) R. A. Layfield, M. Murugesu, *Lanthanides and actinides in molecular magnetism*, John Wiley & Sons, **2015, 336 pp**.

[9] J.-C. G. Bunzli, V. K. Pecharsky, *Handbook on the Physics and Chemistry of Rare Earths: Including Actinides*, Elsevier, **2016, Vol. 50, p. 141**.

[10] J. Long, M. S. Ivanov, V. A. Khomchenko, E. Mamontova, J.-M. Thibaud, J. Rouquette, M. Beaudhuin, D. Granier, R. A. S. Ferreira, L. D. Carlos, B. Donnadieu, M. S. C. Henriques, J. A. Paixão, Y. Guari, J. Larionova, *Science* **2020**, *367*, 671-676.

[11] C. D. S. Brites, A. Millán, L. D. Carlos, in *Handbook on the Physics and Chemistry of Rare Earths, Vol. 49* (Eds.: B. Jean-Claude, P. Vitalij K), Elsevier, **2016**, pp. 339-427.

[12] a) P. Hänninen, H. Härmä, *Lanthanide luminescence: photophysical, analytical and biological aspects, Vol. 7*, Springer Science & Business Media, **2011, 381 pp**; b) J. Yuan, G. Wang, *J. Fluoresc.* **2005**, *15*, 559-568.

[13] M. Ibrahim, B. Hazhirkarzar, A. Dublin, *Magnetic Resonance Imaging (MRI) Gadolinium, Available from: https://www.ncbi.nlm.nih.gov/books/NBK482487/* **2020**.

[14] a) M. Shibasaki, N. Yoshikawa, *Chem. Rev.* **2002**, *102*, 2187-2210; b) H. Pellissier, *Coord. Chem. Rev.* **2017**, *336*, 96-151; c) F. T. Edelmann, *Chem. Soc. Rev.* **2012**, *41*, 7657-7672.

[15] a) W. A. Herrmann, R. Anwander, V. Dufaud, W. Scherer, *Angew. Int. Ed.* **1994**, *33*, 1285-1286; b) J. Annand, H. C. Aspinall, *J. Chem. Soc., Dalton. Trans.* **2000**, 1867-1871; c) J. Annand, H. C. Aspinall, A. Steiner, *Inorg. Chem.* **1999**, *38*, 3941-3943; d) P. L. Arnold, A. J. Blake, S. N. Hall, B. D. Ward, C. Wilson, *J. Chem. Soc., Dalton. Trans.* **2001**, 488-491; e) V. Lorenz, S. Gießmann, Y. K. Gun'ko, A. K. Fischer, J. W. Gilje, F. T. Edelmann, *Angew. Chem. Int. Ed.* **2004**, *43*, 4603-4606; f) V. Lorenz, A. Fischer, F. T. Edelmann, *J. Organomet. Chem.* **2002**, *647*, 245-249; g) G. Wu, Y. Chen, D.-J. Xu, J.-C. Liu, W. Sun, Z. Shen, *J. Organomet. Chem.* **2009**, *694*, 1571-1574; h) V. Lorenz, S. Blaurock, C. G. Hrib, F. T. Edelmann, *Eur. J. Inorg. Chem.* **2010**, *2010*, 2605-2608; i) G.-L. Davies, J. O'Brien, Y. K. Gun'ko, *Scientific Reports* **2017**, *7*, 45862; j) S. Marchesi, F. Carniato, E. Boccaleri, *New J. Chem.* **2014**, *38*, 2480-2485; k) A. R. Willauer, A. M. Dabrowska, R. Scopelliti, M. Mazzanti, *Chem. Commun.* **2020**.

[16] a) V. A. Igonin, S. V. Lindeman, Y. T. Struchkov, O. I. Shchegolikhina, Y. A. Molodtsova, Y. A. Pozdnyakova, A. A. Zhdanov, *Russ. Chem. Bull.* **1993**, *42*, 168-173; b) V. A. Igonin, S. V. Lindeman, Y. T. Struchkov, Y. A. Molodtsova, Y. A. Pozdnyakova, O. I. Shchegolikhina, A. A. Zhdanov, *Russ. Chem. Bull.* **1993**, *42*, 176-181; c) C. Zucchi, O. I. Shchegolikhina, M. Borsari, A. Cornia, G. Gavioli, A. C. Fabretti, E. Rentschler, D. Gatteschi, R. Ugo, R. Psaro, Y. A. Pozdniakova, S. V. Lindeman, A. A. Zhdanov, G. Pályi, *J. Mol. Catal. A: Chem.* **1996**, *107*, 313-321; d) O. I. Shchegolikhina, Y. A. Pozdniakova, S. V. Lindeman, A. A. Zhdanov, R. Psaro, R. Ugo, G. Gavioli, R. Battistuzzi, M. Borsari, T. Rüffer, C. Zucchi, G. Pályi, *J. Organomet. Chem.* **1996**, *514*, 29-35.

[17] H. Masakazu, T. Shinsuke, Y. Takashi, U. Keiji, U. Masafumi, M. Hideyuki, *Chem. Lett.* **2005**, *34*, 1542-1543.

[18] Y.-N. Liu, H.-F. Su, Y.-W. Li, Q.-Y. Liu, Z. Jagličić, W.-G. Wang, C.-H. Tung, D. Sun, *Inorg. Chem.* **2019**, *58*, 4574-4582.

[19] a) J. Long, F. Habib, P.-H. Lin, I. Korobkov, G. Enright, L. Ungur, W. Wernsdorfer, L. F. Chibotaru, M. Murugesu, *J. Am. Chem. Soc.* **2011**, *133*, 5319-5328; b) P.-F. Yan, P.-H. Lin, F. Habib, T. Aharen, M. Murugesu, Z.-P. Deng, G.-M. Li, W.-B. Sun, *Inorg. Chem.* **2011**, *50*, 7059-7065.

[20] C. Y. Chow, H. Bolvin, V. E. Campbell, R. Guillot, J. W. Kampf, W. Wernsdorfer, F. Gendron, J. Autschbach, V. L. Pecoraro, T. Mallah, *Chemical Science* **2015**, *6*, 4148-4159.

[21] a) K. Binnemans, *Chem. Rev.* **2007**, *107*, 2592-2614; b) J.-C. G. Bünzli, S. V. Eliseeva, *Lanthanide luminescence: photophysical, analytical and biological aspects. Hänninen, Pekka, Härmä, Harri, Eds. Berlin Heidelberg: Berlin, Heidelberg, Vol. 7*, Springer Science & Business Media, **2011, pp. 1-45**.

[22] W. T. Carnall, P. R. Fields, K. Rajnak, *J. Chem. Phys.* **1968**, *49*, 4450-4455.

[23] W. Carnell, P. Fields, K. Rajnak, *J. Chem. Phys.* **1968**, *49*, 4447-4449.

[24] a) J.-C. G. Bünzli, C. Piguet, *Chem. Soc. Rev.* **2005**, *34*, 1048-1077; b) S. V. Eliseeva, J.-C. G. Bünzli, *Chem. Soc. Rev.* **2010**, *39*, 189-227.